

Available at [www.sciencedirect.com](http://www.sciencedirect.com)journal homepage: [www.elsevier.com/locate/hydro](http://www.elsevier.com/locate/hydro)

# Study of hydrogen physisorption on nanoporous carbon materials of different origin

M. Armandi<sup>a</sup>, B. Bonelli<sup>a,\*</sup>, K. Cho<sup>b,c</sup>, R. Ryoo<sup>b,c</sup>, E. Garrone<sup>a</sup>

<sup>a</sup> Dipartimento di Scienza dei Materiali e Ingegneria Chimica and INSTM Unit of Torino Politecnico, Politecnico di Torino, Corso Duca degli Abruzzi 24, I-10129 Turin, Italy

<sup>b</sup> Department of Chemistry, Korea Advanced Institute of Science and Technology, Daejeon 305-701, Republic of Korea

<sup>c</sup> Graduate School of Nanoscience and Technology (WCU), Korea Advanced Institute of Science and Technology, Daejeon 305-701, Republic of Korea

## ARTICLE INFO

### Article history:

Received 30 April 2010

Received in revised form

9 December 2010

Accepted 10 January 2011

Available online 12 February 2011

### Keywords:

Nanoporous carbon materials

Carbon replicas

Hydrogen physisorption

CO<sub>2</sub> adsorption

## ABSTRACT

Hydrogen adsorption capabilities of different nanoporous carbon, i.e. amorphous carbons obtained by chemical activation (with KOH) of a sucrose-derived char previously ground by ball milling and carbon replicas of NH<sub>4</sub>-Y and mesocellular silica foam (MSU-F) inorganic templates, were measured and correlated to their porous properties. The porous texture of the prepared carbon materials was studied by means of N<sub>2</sub> and CO<sub>2</sub> adsorption isotherms measured at –196 °C and 0 °C, respectively. Comparison with nanoporous carbons obtained without pre-grinding the sucrose-derived char [12] shows that the ball milling procedure favours the formation of highly microporous carbon materials even at low KOH loadings, having a beneficial effect of the interaction between the char particles and the activating agent. Hydrogen adsorption isotherms at –196 °C were measured in the 0.0–1.1 MPa pressure range, and a maximum hydrogen adsorption capacity of 3.4 wt.% was obtained for the amorphous carbon prepared by activation at 900 °C with a KOH/char weight ratio of 2. Finally, a linear dependence was found between the maximum hydrogen uptake at 1.1 MPa and the samples microporous volume, confirming previous results obtained at –196 °C and sub-atmospheric pressure [12]. Copyright © 2011, Hydrogen Energy Publications, LLC. Published by Elsevier Ltd. All rights reserved.

## 1. Introduction

Highly porous materials that are capable of retaining hydrogen by physisorption are promising adsorbents for applications requiring reversibility of interaction and low temperature operation [1]. To these purposes, zeolites and related microporous solids [2], polymers with intrinsic microporosity (PIMs) [3], metal–organic frameworks (MOFs) [4] and microporous carbons [5–10] are the main kinds of adsorbent investigated.

The two main factors affecting hydrogen storage efficiency by physisorption are the accessible volume of the adsorbent and the strength of the interaction, *e.g.* the standard enthalpy

change of adsorption  $\Delta H^0$ . The latter parameter is of paramount importance when considering the possibility of charge–discharge cycles at accessible temperature: it has been recently reported [11] that for a hydrogen storage delivery cycle at 25 °C with charge at 30 bar and discharge at 1.5 bar, the optimal  $\Delta H^0$  is –15 kJ mol<sup>–1</sup>, an enthalpy value that is out of the range expected for mere dispersion forces. On the other hand, whilst such a strength of interaction may be accessible only by zeolites with highly polarizing cations, these adsorbents present the drawback of a low porous volume and high specific weight. For this reason, the study of highly porous systems with low specific weight, *e.g.* carbon materials, still deserves attention. Activated carbons (ACs) provide the above

\* Corresponding author. Fax: +39 11 5644699.

E-mail address: [barbara.bonelli@polito.it](mailto:barbara.bonelli@polito.it) (B. Bonelli).

**Table 1** Relevant Features of prepared carbon materials.

Sample	Yield <sup>a</sup> %	BETSSA <sup>b</sup> (m <sup>2</sup> g <sup>-1</sup> )	Total porous vol. <sup>c</sup> (cm <sup>3</sup> g <sup>-1</sup> )	V <sub>MPN<sub>2</sub></sub> (cm <sup>3</sup> g <sup>-1</sup> )		V <sub>MPCO<sub>2</sub></sub> (cm <sup>3</sup> g <sup>-1</sup> )		H <sub>2</sub> ads. mass wt.% <sup>d</sup> at 1.1 MPa
				t-plot	NLDFT	DR	NLDFT	
CS09	40	580	0.26	0.21	0.22	0.30	0.21	1.690
CS17	30	1160	0.81	0.36	0.37	0.39	0.31	2.280
CS18	28	1575	0.95	0.48	0.51	0.50	0.34	2.840
CS19	25	1680	1.05	0.48	0.53	0.27	0.31	2.872
CS27	27	1370	0.68	0.50	0.49	0.58	0.39	2.748
CS28	23	1650	0.99	0.57	0.56	0.40	0.32	3.017
CS29	20	1870	1.11	0.64	0.60	0.34	0.30	3.422
C-Y	—	2210	1.17	0.71	0.73	0.15	0.17	3.100
C-MSU-F	41	1000	0.78	0.25	0.30	0.19	0.15	2.339

a Reaction yields calculated as mass of the final product over initial mass of sucrose.

b BET SSA measured by multipoint method in the relative pressure range 0.05–0.15 P/P<sub>0</sub>.

c Total porous volumes as measured from N<sub>2</sub> isotherms at P/P<sub>0</sub> = 0.9.

d H<sub>2</sub> uptake (wt.%) measured at P<sub>H<sub>2</sub></sub> = 1.1 MPa and –196 °C.

properties and are low cost materials that can be obtained by raw sources. Hydrogen physisorption on carbon materials occurs mainly inside micropores [6–8] and it is therefore desirable to improve microporosity in order to enhance hydrogen adsorption capacity. Chemical activation of carbon containing raw materials is a common procedure to prepare ACs with characteristic porous structure, large internal surface area and pore volume. Porous properties of the resultant carbon material depend both on the activation process and on the type of raw material employed. In particular, the use of KOH as activating agent provides highly microporous carbon materials with promising hydrogen storage capabilities [5–7]. In a previous work, highly microporous carbon materials were obtained by chemically activating with KOH a sucrose-derived char [12]: the highest hydrogen uptake, corresponding to 2.5% by weight measured at –196 °C and sub-atmospheric pressure, was obtained with the sample carbonized at 900 °C with a KOH/char mass ratio of 2.0 having the highest microporous volume. In this work, novel nanoporous carbons were synthesized by KOH activation of a sucrose-derived char that was previously ground in a ball mill and performing carbonization at 700 °C, 800 °C or 900 °C. The milling procedure was introduced with the aim of further improving microporosity. For comparison, the carbon replicas of two commercial inorganic templates, namely a NH<sub>4</sub>-Y zeolite and a mesocellular silica foam, were studied.

Hydrogen adsorption capacities at –196 °C of the prepared nanoporous carbons were measured in the 0.0–1.1 MPa pressure range and results were correlated to materials porous architecture as studied by means of N<sub>2</sub> and CO<sub>2</sub> isotherms at –196 °C and 0 °C. CO<sub>2</sub> adsorption is indeed considered a useful tool for characterizing ultra-microporosity (pore width below 0.7 nm) of porous carbon materials [13].

## 2. Experimental

### 2.1. Materials

An aqueous solution containing 5 g sucrose and 0.3 g sulphuric acid was placed into an oven and kept first at 100 °C (3 h) and then at 160 °C (3 h). The obtained char was ground in

a ball mill and afterwards mixed with KOH aqueous solutions (KOH/char weight ratio of either 1 or 2). The dried mixture was carbonized at 700 °C, 800 °C or 900 °C under N<sub>2</sub> (flow rate 350 ml min<sup>-1</sup>, heating rate 5 °C min<sup>-1</sup>). In order to remove potassium-related residues, the resultant products were repeatedly washed with 0.1 M HCl and hot bi-distilled water and dried. The obtained carbon materials will be referred to as CS<sub>x</sub>y, where x stands for the KOH/Char weight ratio and y for the carbonization temperature (7 = 700 °C; 8 = 800 °C; 9 = 900 °C). CS09 reference material was prepared by direct carbonization at 900 °C of the sucrose-derived char, without KOH. Reaction yields of prepared carbon materials were calculated as mass of the final product over starting mass of sucrose (Table 1).

C-Y and C-MSU-F carbon replicas of inorganic templates were synthesized starting from a commercial NH<sub>4</sub>-Y (Zeolite) zeolite and a mesocellular silica foam (MSU-F Sigma–Aldrich), respectively. The former underwent chemical vapor deposition (CVD) of propylene at 800 °C; the latter was impregnated with an acidic solution of sucrose and then carbonized by following a synthesis procedure reported elsewhere [14].

### 2.2. Methods

FESEM pictures were collected on a High Resolution FE-SEM instrument (LEO 1525) equipped with a Gemini Field Emission Column.

For specific surface area (SSA) and pores size measurements, N<sub>2</sub> and CO<sub>2</sub> sorption isotherms were measured at –196 °C and 0 °C, respectively, on samples previously outgassed at 300 °C for at least 4 h, in order to remove water and other atmospheric contaminants (Quantachrome Autosorb 1C instrument). From N<sub>2</sub> isotherms, BET (Brunauer–Emmett–Teller) SSA values were measured by multipoint method within the relative pressure range of 0.05–0.15 P/P<sub>0</sub>; microporous volumes (V<sub>MPN<sub>2</sub></sub>) were calculated according to the t-plot method; cumulative pore volume curves were calculated by applying Non-Local Density Functional Theory (NLDFT) method (kernel for nitrogen adsorption at –196 °C onto carbon slit-pores). From CO<sub>2</sub> isotherms, microporous volumes (V<sub>MPCO<sub>2</sub></sub>) were obtained by applying the Dubinin–Radushkevich (DR) equation, and cumulative pore volume curves were calculated by applying

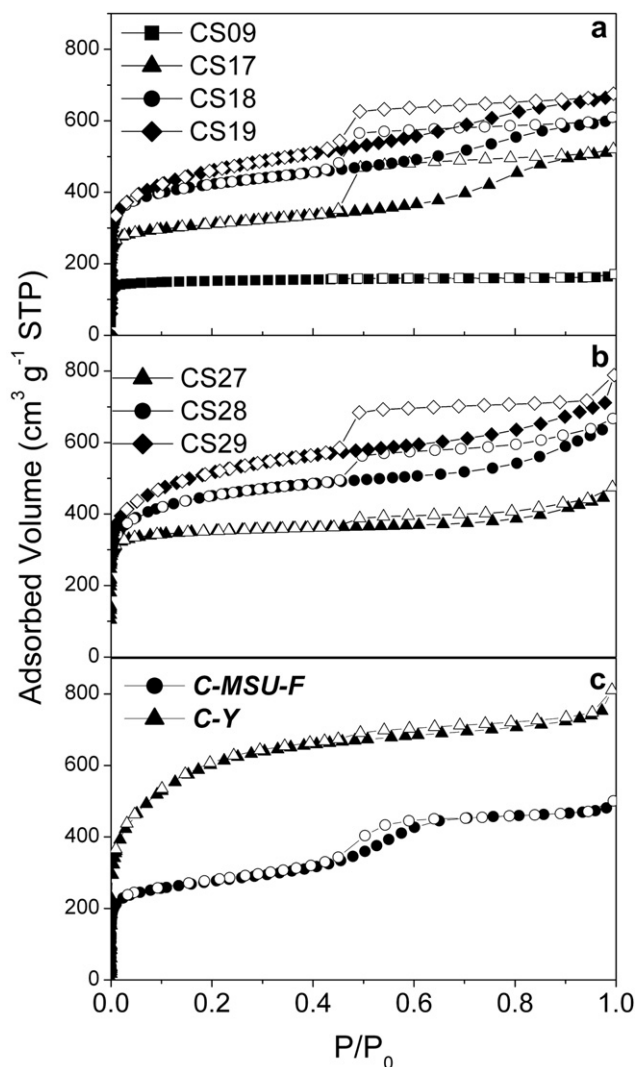


**Fig. 1**  $N_2$  adsorption/desorption isotherms at  $-196\text{ }^\circ\text{C}$  on: (a) CS09 and CS1y samples; (b) CS2y samples; and (c) C-Y and C-MSU-F carbon replicas. Full symbols refer to adsorption branch; white symbols refer to desorption branch.

NLDFT method (kernel for carbon dioxide adsorption at  $0\text{ }^\circ\text{C}$  onto carbon slit-pores).

Hydrogen adsorption isotherms at  $-196\text{ }^\circ\text{C}$  were measured on a laboratory-built volumetric apparatus equipped with an absolute capacitance manometer (MFS Baratron Type 627B), within the pressure range of 0.0–1.1 MPa. Before measurements, 0.5 g carbon sample was outgassed for at least 4 h at  $300\text{ }^\circ\text{C}$ .

### 3. Results and discussion

#### 3.1. Porous properties of the prepared carbon materials as measured by $N_2$ and $CO_2$ adsorption isotherms

**Fig. 1** reports  $N_2$  isotherms  $-196\text{ }^\circ\text{C}$  on CSxy materials (a and b sections) and on carbon replicas (section c), the corresponding BET SSA and porous volumes being reported in **Table 1**.

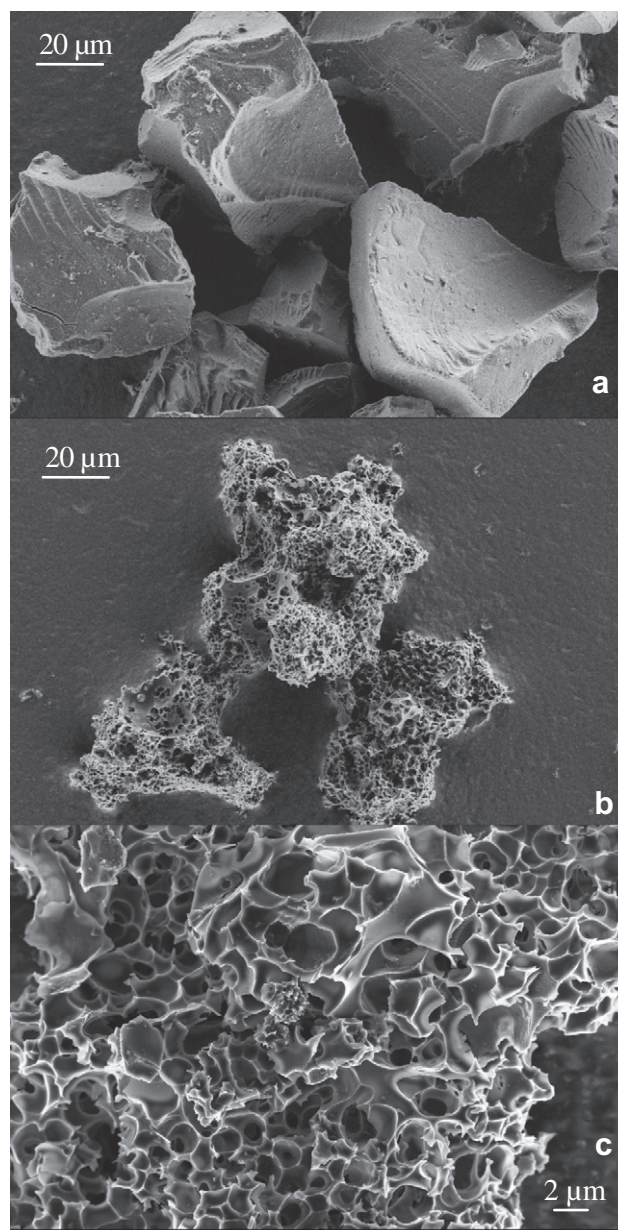


**Fig. 2** FESEM pictures of samples CS18 (a) and CS28 (b and c).

As far as CSxy materials are concerned, CS09 sample presents a Type I isotherm, typical of a microporous adsorbent, and has both the lowest BET SSA and microporous volume (**Table 1**), the isotherm sharp knee being due to a narrow distribution of micropores size. The other CSxy materials showed much higher BET SSA and porous volumes: both values increase with carbonization temperature among samples synthesised with the same KOH/char weight ratio.

With CS1y samples (**Fig. 1a**), isotherm slope smoothly increases in the 0.6–0.8  $P/P_0$  range, indicating a broad distribution of mesopore sizes (in the 5–15 nm range, as calculated according to the BJH method): micropores already present on the reference sample are probably enlarged by KOH attack forming mesopores.

Pore dimensions are enlarged at higher KOH contents (i.e. with CS2y), as evidenced by changes in isotherm shape above  $0.6 P/P_0$ : with CS2y samples, the slope of the adsorption branch increases only above  $0.8–0.9 P/P_0$  values, indicating the occurrence of both larger mesopores and of macropores. The hysteresis loops shape indicates that both meso- and macropores are connected to the outer surface through smaller pores [15,16]: the constant pore emptying at values of  $P/P_0$  around 0.4 observed with all CS samples generally occurs with cavitation-controlled evaporation phenomena in ink-bottle pores with the neck size smaller than a “critical” value of about 2.0 nm [15,16]. Macropore formation for KOH/char weight ratio = 2 is confirmed by FESEM pictures in Fig. 2: CS28 (Fig. 2b and c) shows macropores not detected with CS18 sample (Fig. 2a). A similar trend was observed for samples carbonized at 700 and 900 °C.

The knee of both CS1y and CS2y isotherms becomes rounder at higher carbonization temperatures, indicating the occurrence of a wider and more heterogeneous microporosity.

This result is evidenced by Fig. 3 reporting the cumulative pore volume curves obtained by NLDFT method from  $N_2$  isotherms: the micropore volume increase is accompanied by (i) a decrease of narrower micropores (pore width < 1.0 nm) and (ii) an increase of larger ones. Microporous volumes extrapolated at 2.0 nm and those obtained by the t-plot method are indeed very close (Table 1).

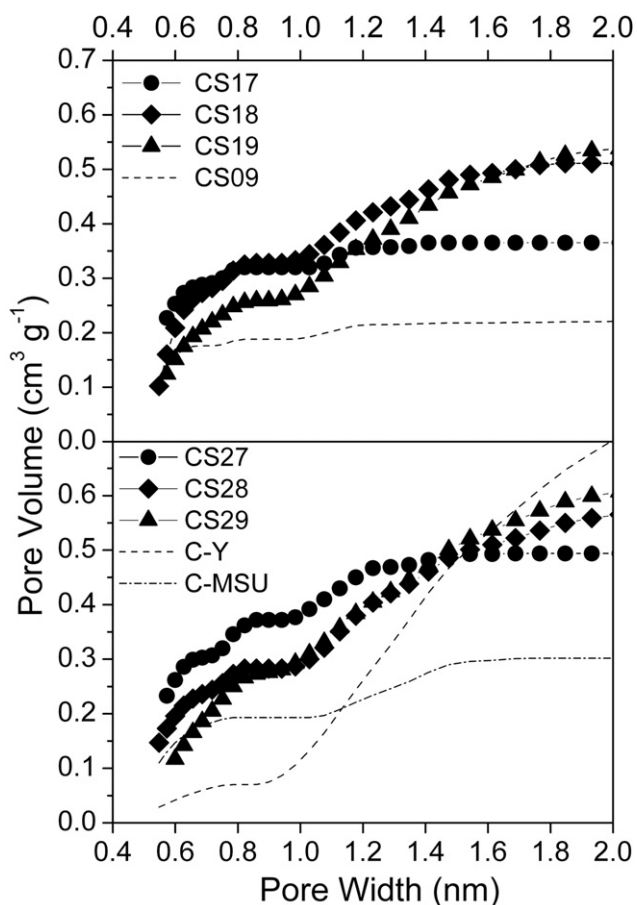


Fig. 3 Cumulative micropore volume curves, as calculated by applying NLDFT method to  $N_2$  isotherms at  $-196$  °C.

CS09 shows a limited porosity that is mainly constituted by pores with diameter smaller than 0.75 nm: such a narrow microporosity is enhanced by KOH activation, especially at low KOH content and carbonization temperature (i.e. CS17, CS18 and CS27 sample). At higher carbonization temperature and KOH content, larger pores are obtained at the expenses of narrower ones, with preferential formation of pores with diameter larger than 0.10 nm. This may be explained by considering the processes occurring during KOH activation (Eqs. (1)–(4)):



Whilst potassium reduction to the elemental state is spontaneous above 570 °C (Eq. (1)) [17,18], higher temperatures

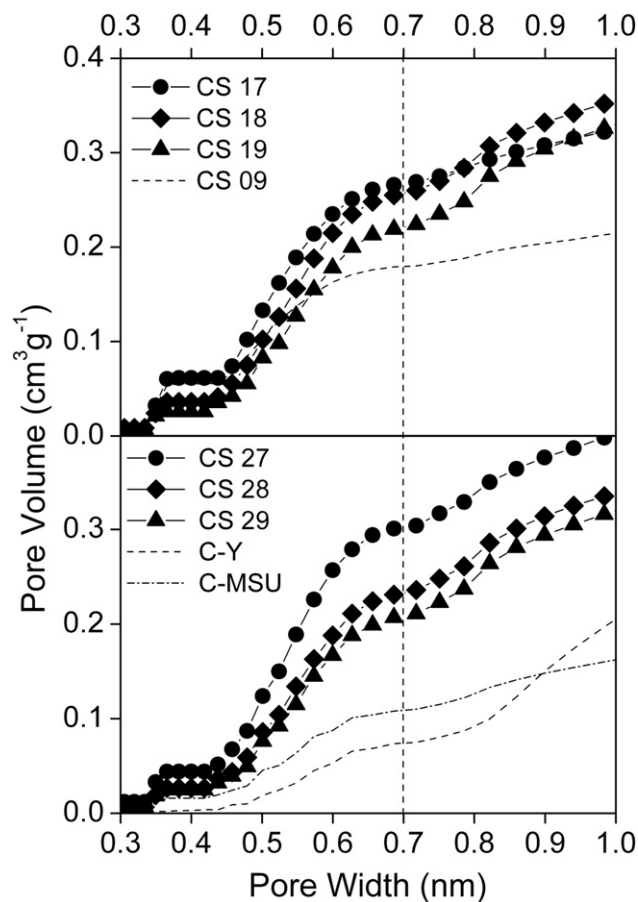
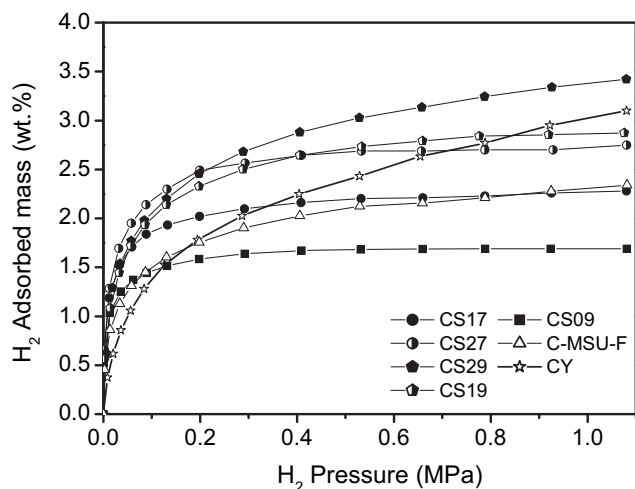


Fig. 4 Cumulative micropore volume curves, as calculated by applying NLDFT method to  $\text{CO}_2$  isotherms at  $0$  °C. Vertical dotted line marks out ultra-microporosity width range.



**Fig. 5** H<sub>2</sub> adsorption isotherms at  $-196\text{ }^{\circ}\text{C}$  in the 0.0–1.1 MPa pressure range on selected samples.

(i.e.  $T > 700\text{ }^{\circ}\text{C}$ ) are required to decompose potassium carbonate and oxide into metallic potassium ( $T_{ev} = 759\text{ }^{\circ}\text{C}$ ) and carbon oxides (Eqs. (2)–(4)). Therefore at higher carbonization temperature and KOH content, larger amounts of CO<sub>2</sub> should form, which can further react with the carbon matrix as in physical activation [18], resulting in the widening of pores diameter and in the lowering of carbon yield.

Comparison with CSxy samples obtained at the same temperature and same KOH/Char ratio without pre-grinding the sucrose-derived char [12] shows that samples reported in this paper present both larger BET SSA and microporous volumes, especially at low KOH/Char ratios, i.e. with CS17 and CS18 samples. The latter sample has both a BET SSA and a microporous volume that are as twice as much those reported in Ref. [12] for a sample obtained in the same conditions, but without milling. This has probably to be ascribed to the formation of smaller char particles that are readily activated by KOH, so obtaining highly microporous carbon materials without the need of larger KOH amounts.

As far as carbon replicas are concerned, Fig. 1c shows that C-Y sample presents a Type I isotherm with a very rounded knee, whereas C-MSU-F sample shows a Type IV isotherm, typical of a mesoporous material with limited microporosity.

As compared to the other samples studied, C-Y has both the highest BET SSA and microporous volume ( $2210\text{ m}^2\text{ g}^{-1}$  and  $0.71\text{ cm}^3\text{ g}^{-1}$ , respectively), as confirmed by the corresponding cumulative pore volume curve (Fig. 3) showing that most of its microporosity is constituted by pore larger than 1.0 nm.

Cumulative pore volume curves obtained by applying the NLDFT method to CO<sub>2</sub> isotherms (Fig. 4) allow a detailed study of samples micropores population to be carried out: with CSxy samples, two steps are observed in the ultra-micropores range (at 0.3–0.4 and 0.4–0.7 nm pore width, respectively), which decrease with increasing carbonization temperature, regardless of the KOH/char ratio.

With the exception of CS09 and CS17, the other CSxy samples shows a third step at about 0.8 nm: to this respect, it

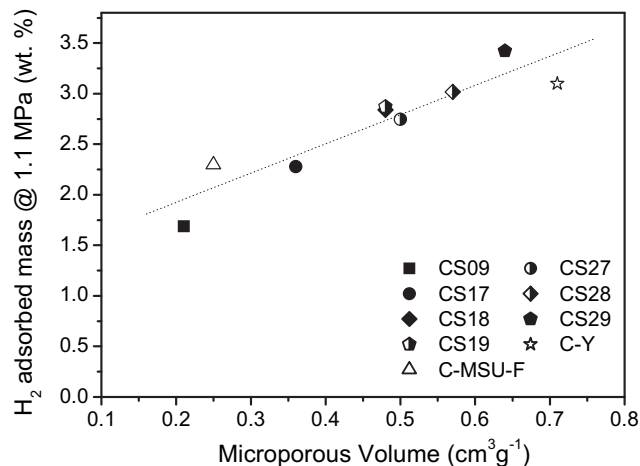


**Fig. 6** Linear correlation between the maximum H<sub>2</sub> uptake at  $-196\text{ }^{\circ}\text{C}$  and 1.1 MPa and the microporous volume (from the t-plot method) of prepared carbon materials.

must be observed that 0.9–1.0 nm pore width is the upper limit of sensitivity to pores size for sub-atmospheric CO<sub>2</sub> adsorption at 0 °C [19] and therefore, microporous volume values ( $V_{MPCO_2}$ ) reported in Table 1 were extrapolated from cumulative pore volume curves at 0.95 nm.

Finally, unlike CSxy samples, both carbon replicas showed very limited ultra-microporosity.

Microporous volumes were also calculated by applying the DR equation to CO<sub>2</sub> isotherms (Table 1): despite some discrepancies, the values provided by the two methods (i.e. DR and NLDFT) vary with the same trend.

### 3.2. Hydrogen physisorption

Fig. 5 reports selected H<sub>2</sub> isotherms taken at  $-196\text{ }^{\circ}\text{C}$  in the 0–1.1 MPa pressure range; maximum uptakes at 1.1 MPa measured as percentages by weight of adsorbed hydrogen over sample mass being gathered in Table 1. Isotherm analysis shows that, in the adopted experimental conditions, the highest uptake corresponding to 3.4% by weight was reached on CS29 sample. Such result is comparable with (i) some of the best literature data concerning hydrogen adsorption capabilities of different carbon materials (i.e. zeolite carbon replicas and activated carbons), as measured at  $-196\text{ }^{\circ}\text{C}$  and 1.1 MPa [7,9,20,21], for which a maximum H<sub>2</sub> uptake of 4.0% by weight is reported at 1.1 MPa [21] and with (ii) previous results obtained at  $-196\text{ }^{\circ}\text{C}$  and sub-atmospheric pressure on CSxy samples obtained without grinding [12].

In previous works [5,6,12], it was shown that H<sub>2</sub> uptake on porous carbons increases with increasing microporous volume, rather than with BET SSA, as reported in the literature for several other types of adsorbents [22–25]. Fig. 6 reports maximum adsorbed volumes at 1.1 MPa and  $-196\text{ }^{\circ}\text{C}$  versus  $V_{MPN_2}$  values, as calculated according to the t-plot method. In agreement with previous findings, a good linear correlation is found, which definitely points out to the crucial role of microporosity in H<sub>2</sub> adsorption, also at high-pressure range.

As far as isotherm shape is concerned, it is noteworthy that samples showing highest hydrogen uptake (*i.e.* CS29 and C-Y) did not reach a plateau in H<sub>2</sub> adsorption at 1.1 MPa, showing that at higher pressures higher hydrogen capacities would be possible. Actually, isotherms shape is strictly related to micropores size distribution [23–27], and indeed both samples showed a large amount of wider micropores, which requires high pressure to be saturated. On the other hand, isotherms of samples with larger  $V_{MPCO_2}$  values, like CS27 and CS18 (isotherm not reported in the figure for clarity), show a steeper increase in hydrogen adsorption at relatively low pressures, but reach a plateau at about 0.3–0.4 MPa.

In summary, hydrogen adsorption occurs basically inside micropores: higher uptakes are expected at higher pressures, at which the contribution of larger micropores should become more relevant, as previously reported by both theoretical and experimental studies [28–30].

#### 4. Conclusions

Novel CSxy microporous carbons were prepared by a facile method consisting of the chemical activation with KOH of a sucrose-derived char that was pre-ground by ball milling in order to improve microporosity, an important parameter affecting hydrogen physisorption on porous systems. The effects of the amount of KOH used, the carbonization temperature and the ball milling procedure on carbon material porosity were studied, as well. For comparison, C-Y and C-MSU-F carbon replicas were obtained from two commercial inorganic matrices, a NH<sub>4</sub>-Y and a MSU-F silica foam, respectively. With CSxy systems, an increase of microporous volume was observed with both the carbonization temperature and the amount of KOH used; comparison with CSxy samples obtained without milling, as described in a previous paper [12], showed that the ball milling procedure probably favours the formation of smaller particles of char, readily activated by KOH. This effect results in larger values of both BET SSA and microporous volume, especially at low KOH loading. This is important since it is shown that it is possible to obtain highly microporous carbon materials, suitable for hydrogen physisorption, by using smaller amounts of KOH when the char is previously ball milled. C-Y and C-MSU-F resulted to be mostly microporous and mesoporous material, respectively.

The highest hydrogen uptake at 1.1 MPa and –196 °C was shown by CS29 sample obtained with a KOH/char = 2 and carbonized at 900 °C, the related adsorbed hydrogen volume being 376 cm<sup>3</sup> g<sup>-1</sup>, corresponding to ~3.4 wt.%. The obtained result was comparable with the best literature data obtained in the same experimental conditions on other carbon materials and with previous data obtained on similar materials at sub-atmospheric pressure [12].

A detailed study of the porous architecture of the prepared materials allowed us to figure out some relevant porous properties, finally affecting their H<sub>2</sub> adsorption capacities, especially as far as microporosity is concerned. The latter parameter has indeed a crucial role towards hydrogen physisorption on porous carbon materials not only at low H<sub>2</sub>

pressures [12], but also when higher pressures are adopted, as in this work.

Finally, with respect to C-Y and C-MSU-F carbon replicas, the facile synthesis of CSxy carbons open the possibility to obtain highly microporous materials with good hydrogen adsorption properties, without the need for a more complicated and expensive casting procedure and to improve microporosity by pre-grinding the sucrose-derived char without the need of using high KOH amounts.

#### Acknowledgments

Financial supports are acknowledged from Regione Piemonte (FESR Project STEPS) and MiUR (Ministero dell'Università e della Ricerca – FISR Project Vettore Idrogeno) in Italy, and National Research Foundation (National Honor Scientist Program 20100029665 and World Class University Program R31-2008-000-10071-0) in Korea.

#### REFERENCES

- [1] Van den Berg A, Otero Areán C. Materials for hydrogen storage: current research trends and perspectives. *Chem Commun*; 2008:668–81.
- [2] Palomino GT, Bonelli B, Otero Areán C, Parra JB, Carayol MRL, Armandi M, et al. Thermodynamics of hydrogen adsorption on calcium exchanged faujasite-type zeolites. *Int J Hydrogen Energy* 2009;34:4371–8.
- [3] Budd PM, Butler A, Selbie J, Mahmood K, McKeown NB, Ghanem B, et al. The potential of organic polymer-based hydrogen storage materials. *Phys Chem Chem Phys* 2007;9: 1802–8.
- [4] Collins DJ, Zhou HC. Hydrogen storage in metal–organic frameworks. *J Mater Chem* 2007;17:3154–60.
- [5] Armandi M, Bonelli B, Karaindrou EI, Otero Areán C, Garrone E. Post-synthesis modifications of SBA-15 carbon replicas: improving hydrogen storage by increasing microporous volume. *Catal Today* 2008;138:244–8.
- [6] Armandi M, Bonelli B, Otero Areán C, Garrone E. Role of microporosity in hydrogen adsorption on templated nanoporous carbons. *Micropor Mesopor Mater* 2008;112: 411–8.
- [7] Jorda-Beneyto M, Lozano-Castello D, Suarez-Garcia F, Cazorla-Amoros D, Linares-Solano A. Advanced activated carbon monoliths and activated carbons for hydrogen storage. *Micropor Mesopor Mater* 2008;112:235–42.
- [8] Texier-Mandoki N, Dentzer J, Piquero T, Saadallah S, David P, Vix-Guterl C. Hydrogen storage in activated carbon materials: role of the nanoporous texture. *Carbon* 2004;42: 2744–7.
- [9] Yang Z, Xia Y, Sun X, Mokaya R. Preparation and hydrogen storage properties of zeolite-templated carbon materials nanocast via chemical vapor deposition: effect of the zeolite template and nitrogen doping. *J Phys Chem B* 2006;110: 18424–31.
- [10] Zhao XB, Xiao B, Fletcher AJ, Thomas KM. Hydrogen adsorption on functionalized nanoporous activated carbons. *J Phys Chem B* 2005;109:8880–8.
- [11] Garrone E, Bonelli B, Areán CO. Enthalpy–entropy correlation for hydrogen adsorption on zeolites. *Chem Phys Lett* 2008;456:68–70.

- [12] Armandi M, Bonelli B, Geobaldo F, Garrone E. Nanoporous carbon materials obtained by sucrose carbonization in the presence of KOH. *Micropor Mesopor Mater* 2010;132:414–20.
- [13] Jagiello J, Thommes M. Comparison of DFT characterization methods based on N<sub>2</sub>, Ar, CO<sub>2</sub>, and H<sub>2</sub> adsorption applied to carbons with various pore size distributions. *Carbon* 2004;42:1227–32.
- [14] Armandi M, Bonelli B, Bottero I, Otero Areán C, Garrone E. Synthesis and characterization of ordered porous carbons with potential applications as hydrogen storage media. *Micropor Mesopor Mater* 2007;103:150–7.
- [15] Neimark AV, Lin Y, Ravikovitch PI, Thommes M. Quenched solid density functional theory and pore size analysis of micro-mesoporous carbons. *Carbon* 2009;47:1617–28.
- [16] Ravikovitch PI, Neimark AV. Experimental confirmation of different mechanisms of evaporation from ink-bottle type pores: equilibrium, pore blocking, and cavitation. *Langmuir* 2002;18(25):9830–7.
- [17] Figueroa-Torres MZ, Robau-Sanchez A, de la Torre-Saenz L, Aguilar-Elguezabal A. Hydrogen adsorption by nanostructured carbons synthesized by chemical activation. *Micropor Mesopor Mater* 2007;98:89–93.
- [18] Lozano-Castello D, Calo JM, Cazorla-Amoròs D, Linares-Solano A. Carbon activation with KOH as explored by temperature programmed techniques and the effects of hydrogen. *Carbon* 2007;45:2529–36.
- [19] Vishnyakov A, Ravikovitch PI, Neimark AV. Molecular level models for CO<sub>2</sub> sorption in nanopores. *Langmuir* 1999;15:8736–42.
- [20] Guan C, Wang K, Yang C, Zhao XS. Characterization of a zeolite-templated carbon for H<sub>2</sub> storage application. *Micropor Mesopor Mat* 2009;118:503–7.
- [21] Panella B, Hirscher M, Roth S. *Carbon* 2005;43:2209–14.
- [22] Züttel A. Materials for hydrogen storage. *Mater Today* 2003;6:24–33.
- [23] Zecchina A, Bordiga S, Vitillo JG, Ricchiardi G, Lamberti C, Spoto G, et al. Role of exposed metal sites in hydrogen storage in MOFs. *J Am Chem Soc* 2005;127:6361–6.
- [24] Rowsell JLC, Millward AR, Park KS, Yaghi OM. Hydrogen sorption in functionalized metal-organic frameworks. *J Am Chem Soc* 2004;126:5666–7.
- [25] Nijkamp MG, Raaymakers J, van Dillen AJ, de Jong KP. Hydrogen storage using physisorption – materials demands. *Appl Phys A* 2001;72:619–23.
- [26] Kowalczyk P, Holyst R, Terzyk AP, Gauden PA. State of hydrogen in idealized carbon slitlike nanopores at 77 K. *Langmuir* 2006;22:1970–2.
- [27] Jagiello J, Ansòn A, Martínez MT. DFT-based prediction of high-pressure H<sub>2</sub> adsorption on porous carbons at ambient temperatures from low-pressure adsorption data measured at 77 K. *J Phys Chem B* 2006;110:4531–4.
- [28] de la Casa-Lillo MA, Lamari-Darkrim F, Cazorla-Amoròs D, Linares-Solano A. Hydrogen storage in activated carbons and activated carbon fibers. *J Phys Chem B* 2002;106:10930–4.
- [29] Jorda-Beneyto M, Suarez-Garcì S, Lozano-Castello D, Cazorla-Amoròs D, Linares-Solano A. Hydrogen storage on chemically activated carbons and carbon nanomaterials at high pressures. *Carbon* 2007;45:293–303.
- [30] Ansòn A, Jagiello J, Parra JB, Sanjuàn ML, Benito AM, Maser WK, et al. Porosity, surface area, surface energy, and hydrogen adsorption in nanostructured carbons. *J Phys Chem B* 2004;108:15820–6.